

(12)

ESD-TR-82-398

MTR-8533

GRATING LOBE CONSIDERATIONS FOR THE APATS ARRAY

By
G. A. ROBERTSHAW

DECEMBER 1982

Prepared for
DEPUTY FOR MISSION SUPPORT SYSTEMS
ELECTRONIC SYSTEMS DIVISION
AIR FORCE SYSTEMS COMMAND
UNITED STATES AIR FORCE
Hanscom Air Force Base, Massachusetts

AD A 122583



DTIC
ELECTE
DEC 20 1982
B

THIS FILE COPY

Approved for public release,
distribution unlimited

Project No. 4290
Prepared by
THE MITRE CORPORATION
Bedford, Massachusetts
Contract No. F19628-82-C-0001

When U.S. Government drawings, specifications, or other data are used for any purpose other than a definitely related government procurement operation, the government thereby incurs no responsibility nor any obligation whatsoever; and the fact that the government may have formulated, furnished, or in any way supplied the said drawings, specifications, or other data is not to be regarded by implication or otherwise, as in any manner licensing the holder or any other person or corporation, or conveying any rights or permission to manufacture, use, or sell any patented invention that may in any way be related thereto.

Do not return this copy. Retain or destroy.

REVIEW AND APPROVAL

This technical report has been reviewed and is approved for publication.



MICHAEL ZYMARIS/GS-13
Project Engineer

FOR THE COMMANDER



JAMES CHASTONG, Major, USAF
Project Manager

UNCLASSIFIED

SECURITY CLASSIFICATION OF THIS PAGE (When Data Entered)

REPORT DOCUMENTATION PAGE		READ INSTRUCTIONS BEFORE COMPLETING FORM
1. REPORT NUMBER ESD-TR-82-398	2. GOVT ACCESSION NO. A122583	3. RECIPIENT'S CATALOG NUMBER
4. TITLE (and Subtitle) GRATING LOBE CONSIDERATIONS FOR THE APATS ARRAY		5. TYPE OF REPORT & PERIOD COVERED
7. AUTHOR(s) G. A. ROBERTSHAW		6. PERFORMING ORG. REPORT NUMBER MTR-8533
9. PERFORMING ORGANIZATION NAME AND ADDRESS The MITRE Corporation P. O. Box 208 Bedford, MA 01730		8. CONTRACT OR GRANT NUMBER(s) F19628-82-C-0001
11. CONTROLLING OFFICE NAME AND ADDRESS Deputy for Mission Support Systems Electronic Systems Division, AFSC Hanscom AFB, MA 01731		10. PROGRAM ELEMENT, PROJECT, TASK AREA & WORK UNIT NUMBERS Project No. 4290
14. MONITORING AGENCY NAME & ADDRESS (if different from Controlling Office)		12. REPORT DATE DECEMBER 1982
		13. NUMBER OF PAGES 42
		15. SECURITY CLASS. (of this report) UNCLASSIFIED
		15a. DECLASSIFICATION DOWNGRADING SCHEDULE
16. DISTRIBUTION STATEMENT (of this Report) Approved for public release; distribution unlimited.		
17. DISTRIBUTION STATEMENT (of the abstract entered in Block 20, if different from Report)		
18. SUPPLEMENTARY NOTES		
19. KEY WORDS (Continue on reverse side if necessary and identify by block number) ANTENNA APATS ARRAY GRATING LOBE		
20. ABSTRACT (Continue on reverse side if necessary and identify by block number) The spacing of the elements which comprise a phased array antenna, such as APATS, is usually selected to prevent the occurrence of grating lobes when the main beam is steered to any position within the specified field of view. Array designers may desire to use the maximum element separation consistent with grating lobe constraints in order to minimize the number of elements needed to fill a given aperture, and thereby reduce antenna cost and complexity. Analysis founded upon reciprocal (Fourier) space construction concepts commonly (over)		

UNCLASSIFIED

SECURITY CLASSIFICATION OF THIS PAGE(When Data Entered)

20. (Concluded)

employed by crystallographers is used to determine the optimum element lattice for planar arrays having the nominal specified APATS field of view and boresight elevations of 10° and 15° respectively. The theory is discussed in sufficient detail and generality to permit application to other array systems.

UNCLASSIFIED

SECURITY CLASSIFICATION OF THIS PAGE(When Data Entered)

ACKNOWLEDGEMENTS

This document has been prepared by The MITRE Corporation under Project 4290, Contract F19628-82-C-0001. The contract is sponsored by the Electronic Systems Division, Air Force Systems Command, Hanscom Air Force Base, Massachusetts.

Accession For		
NTIS	<input checked="" type="checkbox"/>	
DTIC	<input type="checkbox"/>	
Special	<input type="checkbox"/>	
Accession Codes		
Dist. and/or		
Dist.	Special	
A		



TABLE OF CONTENTS

<u>Section</u>	<u>Page</u>
LIST OF ILLUSTRATIONS	4
LIST OF TABLES	4
I INTRODUCTION	5
II BASIC CONCEPTS	6
III ANALYSIS AND RESULTS FOR APATS	20
IV CONCLUSIONS	34
LIST OF REFERENCES	36
APPENDIX: RECIPROCAL SPACE AND FOURIER SERIES	37

LIST OF ILLUSTRATIONS

<u>Figure</u>		<u>Page</u>
1	PHASE FACTOR GEOMETRY	7
2	RECIPROCAL LATTICE FOR 2-D ARRAY	11
3	GRATING LOBE CONDITION	13
4	OPTIMUM RECTANGULAR RECIPROCAL LATTICE FOR CONICAL SCAN	15
5	OPTIMUM TRIANGULAR RECIPROCAL LATTICE FOR CONICAL SCAN	17
6	RECIPROCAL SPACE CONSTRUCTION FOR 10° BORESIGHT ELEVATION	21
7	T1 SPACE LATTICE	25
8	T2 SPACE LATTICE	26
9	RECIPROCAL SPACE CONSTRUCTION FOR 15° BORESIGHT ELEVATION	29

LIST OF TABLES

<u>Table</u>		<u>Page</u>
1	LATTICE CHARACTERISTICS FOR APATS FIELD OF VIEW	28
2	ELEMENT COUNT VERSUS LATTICE TYPE	35

SECTION I
INTRODUCTION

The nominal APATS field of view, for an array antenna with a horizontal boresight, is $\pm 60^\circ$ in azimuth and between 45° and -15° in elevation; however, the contractor may modify these numbers as a result of system trade-off studies. The spacing of the array's elements should be chosen such that grating lobes do not occur when the main beam is steered within the boundaries of the specified field of view. In addition, it is desirable to space the elements as far apart as possible, in the context of the grating lobe constraint, in order to minimize array cost and complexity, since larger separations permit a given aperture to be filled using fewer elements.

Determination of an optimum or near optimum element lattice for two dimensional arrays is expedited by a procedure which incorporates the very elegant concept of the "reciprocal lattice*" (RL) which is employed extensively in crystallography and solid state physics. Basic RL concepts are covered in the next section, while specific application of this type of analysis to APATS is deferred until Section III. A brief conclusion section completes this work.

* This formation is due to J. Willard Gibbs. A basic introduction to reciprocal space concepts can be found in Introduction to Solid State Physics, C. Kittel (J. Wiley and Sons, 1971) p. 56-69.

SECTION II

BASIC CONCEPTS

A 3-D space lattice of point isotropic scatterers can be described by integral combinations of three primitive translation vectors. The vector from the origin lattice site ($n = 0, p = 0, m = 0$) to the site designated by the integers n, p and m is therefore,

$$\vec{R}_{npm} = n\vec{a} + p\vec{b} + m\vec{c} \quad (1)$$

in which \vec{a}, \vec{b} and \vec{c} are a particular set of primitive translation vectors often chosen for convenience. The position vector of equation (1) ranges over the lattice as the indices are varied. If the lattice is excited by a plane wave of wave vector \vec{k} , each site produces an outgoing spherical wave, since it is assumed that the scatterers are isotropic. For elastic scattering these waves may add constructively to produce an outgoing plane wave or waves characterized by \vec{k}', \vec{k}'' etc. such that,

$$|\vec{k}| = |\vec{k}'| = |\vec{k}''| = 2\pi/\lambda \quad (2)$$

Consider an incident, \vec{k} , and outgoing, \vec{k}' , plane wave. The phase of the wavelet scattered from the lattice at \vec{R}_{npm} relative to that scattered from the point at the origin is,

$$\begin{aligned} \phi_{npm}(\vec{k}, \vec{k}') &= \vec{k} \cdot \vec{R}_{npm} - \vec{k}' \cdot \vec{R}_{npm} \\ &= (\vec{k} - \vec{k}') \cdot \vec{R}_{npm} = \Delta\vec{k} \cdot \vec{R}_{npm} \end{aligned} \quad (3)$$

as illustrated for a 2-D lattice in Figure 1. If \vec{k}' is a scattered plane wave due to reinforcement of the wavelets from all lattice

sites, the phase factor of equations (3) must be some integral multiple of 2π radians for each set of (n, p, m) values,

$$\phi_{npm}(\vec{k}, \vec{k}') = 2\pi\eta_{npm} \quad (\eta_{npm} = \text{integer or } 0) \quad (4)$$

or, using equations (3) and (1),

$$\vec{k} \cdot \vec{R}_{npm} = n(\vec{\Delta k} \cdot \vec{a}) + p(\vec{\Delta k} \cdot \vec{b}) + m(\vec{\Delta k} \cdot \vec{c}) = 2\pi\eta_{npm} \quad (5)$$

and it is evident that this equation is satisfied for all allowed values of n, p and m if and only if the "Laue Conditions For Diffraction Maxima" are simultaneously satisfied:

$$\vec{\Delta k} \cdot \vec{a} = 2\pi h, \quad h = \dots 1, 0, 1, \dots \quad (6a)$$

$$\vec{\Delta k} \cdot \vec{b} = 2\pi k, \quad k = \dots 1, 0, 1, \dots \quad (6b)$$

$$\vec{\Delta k} \cdot \vec{c} = 2\pi l, \quad l = \dots 1, 0, 1, \dots \quad (6c)$$

These equations, interestingly, are satisfied if $\vec{\Delta k}$ is given by,

$$\vec{\Delta k} = h\vec{A} + k\vec{B} + l\vec{C} = \vec{G}_{hkl} \quad (7)$$

in which,

$$\vec{A} = \frac{2\pi(\vec{b} \times \vec{c})}{\vec{a} \cdot (\vec{b} \times \vec{c})} \quad (8a)$$

$$\vec{B} = \frac{2\pi(\vec{c} \times \vec{a})}{\vec{a} \cdot (\vec{b} \times \vec{c})} \quad (8b)$$

$$\vec{C} = \frac{2\pi(\vec{a} \times \vec{b})}{\vec{a} \cdot (\vec{b} \times \vec{c})} \quad (8c)$$

are primitive reciprocal lattice vectors* which are constructed from the primitive space lattice vectors, and have units of inverse length. The magnitude of the vector triple product in the denominator of equations (8) is the volume of the primitive unit cell of the space lattice. Each point of the reciprocal lattice specified by h, k, l indices represents an allowed diffraction maximum due to scattering from the corresponding space lattice. If a single, isotropic scatterer is located at each space lattice point, the diffracted beam will exist and be characterized by \vec{k}' such that,

$$\vec{k}'_{hkl} = \vec{k} - \vec{G}_{hkl} \quad (9)$$

in which the diffracted wave vector is labeled by the (h,k,l) indices of the reciprocal lattice vector. The inverse transformation should also be noted⁺,

$$\vec{a} = \frac{2\pi(\vec{B} \times \vec{C})}{\vec{A} \times \vec{B} \cdot \vec{C}} \quad (10a)$$

$$\vec{b} = \frac{2\pi(\vec{C} \times \vec{A})}{\vec{A} \times \vec{B} \cdot \vec{C}} \quad (10b)$$

$$\vec{c} = \frac{2\pi(\vec{A} \times \vec{B})}{\vec{A} \times \vec{B} \cdot \vec{C}} \quad (10c)$$

* Actually psuedo vectors, but this is irrelevant if coordinates system of one handedness is used consistently.

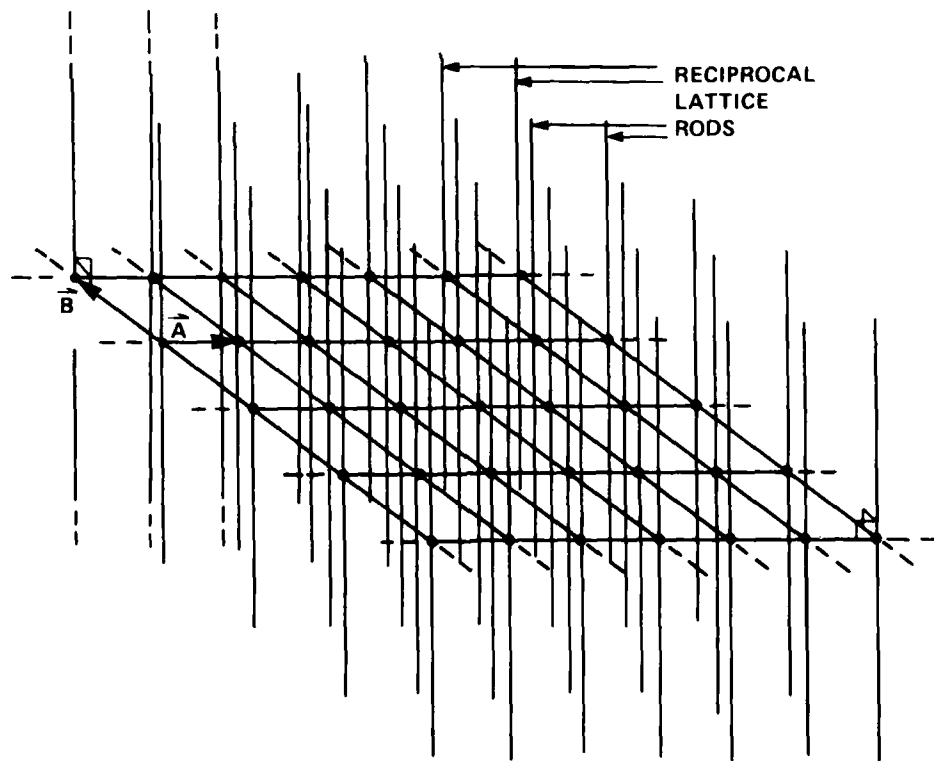
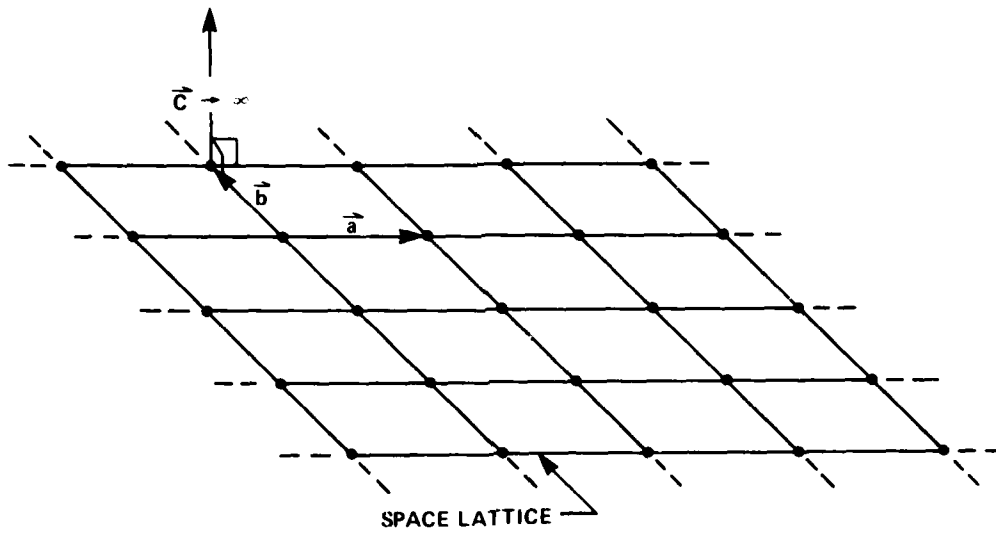
⁺ Since \vec{a} , \vec{b} and \vec{c} , as defined here, are pseudo vectors, the inverse transformation is not valid if the coordinates system is inverted.

and will be used later in the analysis. To apply the above diffraction theory concepts to a planar array, it is necessary to determine the reciprocal lattice for 2-D periodic arrangements of scatterers. Imagine an infinite collection of identical 2-D lattices stacked to form a 3-D lattice such that the lattice points are in vertical registry, i.e., the points of one array are directly above those of its lower neighbor. If the vertical separation between the arrays is allowed to increase without limit, only one array, i.e. the one assumed to be stationary with respect to a hypothetical observer, remains. In reciprocal space, however, the reciprocal lattice points corresponding to the separate arrays move closer together as the space lattice is expanded, and, in the limit of infinite spacial separation, the reciprocal lattice points coalesce into rods. If \vec{c} is the array separation vector which is increased without limit, the rods pass through the reciprocal lattice points given by,

$$\vec{C}_{hk} = h\vec{A} + k\vec{B} \quad (11)$$

and are perpendicular to plane determined by \vec{A} and \vec{B} (i.e, along \vec{C}), as illustrated in figure 2 for a rectangular array. If the reciprocal lattice of the array is viewed along the rods, it appears as the 2-D lattice of equation (11); however, it must be remembered that it actually occupies three dimensions.

An array beam scanned to array azimuth (ϕ) and elevation (θ), and formed at a wavelength, λ , is represented by \vec{k} in the previous analysis. The wave vector is conveniently expressed in terms of its direction cosine angles, α , β , and γ with respect to the array x (horizontal), y and z (boresight) axes respectively:



IA-63,935

Figure 2. RECIPROCAL LATTICE FOR 2-D ARRAY

$$\begin{aligned}\vec{k} &= k_x \hat{X} + k_y \hat{Y} + k_z \hat{Z} \\ &= (2\pi/\lambda)(\cos\alpha \hat{X} + \cos\beta \hat{Y} + \cos\gamma \hat{Z})\end{aligned}\quad (12)$$

The direction cosines are related to the array azimuth and elevation by,

$$\cos\alpha = \cos\theta \sin\phi, \quad \cos\beta = \sin\theta, \quad \cos\gamma = \cos\theta \cos\phi \quad (13)$$

The grating lobes are identified with the primed wave vectors which correspond to diffraction maxima, and can be identified by the h, k indices of their associated reciprocal lattice rods.

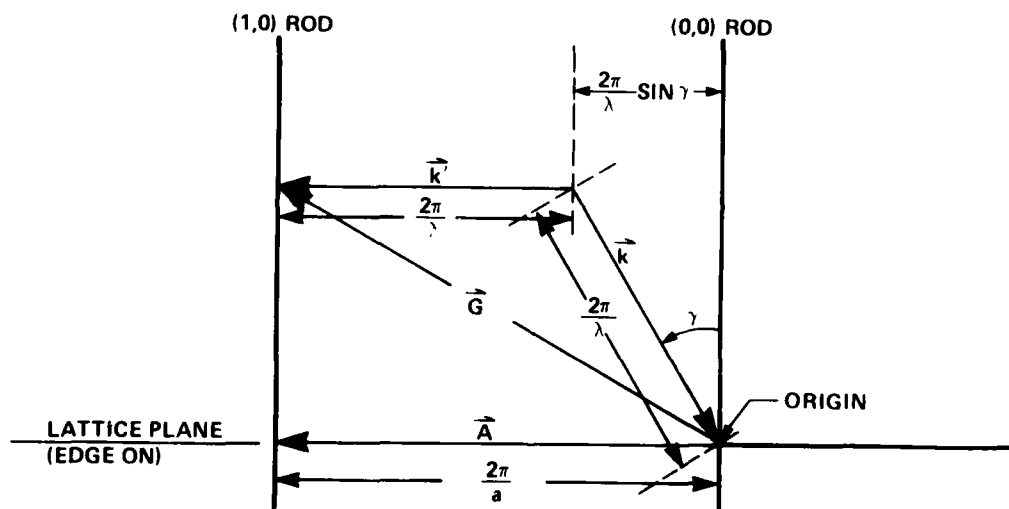
For simplicity, consider first only the reciprocal lattice rods lying in one plane along \vec{A} . The origin of reciprocal space is placed at an arbitrary point along one rod and the head of \vec{k} is placed at this point. The array beam, represented by \vec{k} , is steered off boresight by an angle γ in the plane of the rods, and first grating lobe will occur when \vec{k} is scanned off boresight enough to enable \vec{k}' to contact an adjacent rod, as shown in figure 3. The incipient grating lobe emerges parallel to the array, and by construction equation (9) is satisfied. More specifically,

$$|\vec{k}| \sin \gamma + |\vec{k}'| = |\vec{A}| = 2\pi/a \quad (14)$$

or,

$$a = \lambda(1 + \sin \gamma)^{-1} \quad (15)$$

expresses the element separation (referred to as optimum here) at which the grating lobe peak direction is parallel to the array face. For example, if $\gamma = 60^\circ$, the separation, a , can be as large as 0.536λ before the grating lobe peak emerges from the plane of the array (in the \vec{A} direction).



IA-63,939

Figure 3. GRATING LOBE CONDITION

When considering grating lobe emergence in the whole plane of the array, the reciprocal lattice should be viewed along the rods to produce a 2-D lattice perspective.

In figure 4 a 2-D generalization of the construction of figure 3 is illustrated. The inner circle represents the projection of the tail of \vec{k} onto a plane perpendicular to the reciprocal lattice rods for the boundary of a conical scan volume of half angle γ about the array boresight, which is parallel to the rods. The outer concentric circle represents the projection of the outer boundary of the set of vectors obtained by subtracting \vec{k} from potential grating lobe wavevectors, \vec{k}' . The rectangular reciprocal lattice which corresponds to the optimum space lattice is found by placing a rectangular array of rods about the outer boundary in such a manner that the rods closest to the origin contact the boundary. When a rod touches the boundary, equation (9) is satisfied by a grazing (parallel to the array) grating lobe peak which is directed from the origin rod to the point of contact. For the conical scan volume the optimum rod lattice is obviously square, as illustrated in figure 4, and has primitive basis vectors,

$$\vec{A} = (2\pi/\lambda)(1 + \sin\gamma) \hat{X} \quad (16a)$$

$$\vec{B} = (2\pi/\lambda)(1 + \sin\gamma) \hat{Y} \quad (16b)$$

which corresponds to the space lattice basis,

$$\vec{a} = \lambda(1 + \sin\gamma)^{-1} \hat{X} \quad (17a)$$

$$\vec{b} = \lambda(1 + \sin\gamma)^{-1} \hat{Y} \quad (17b)$$

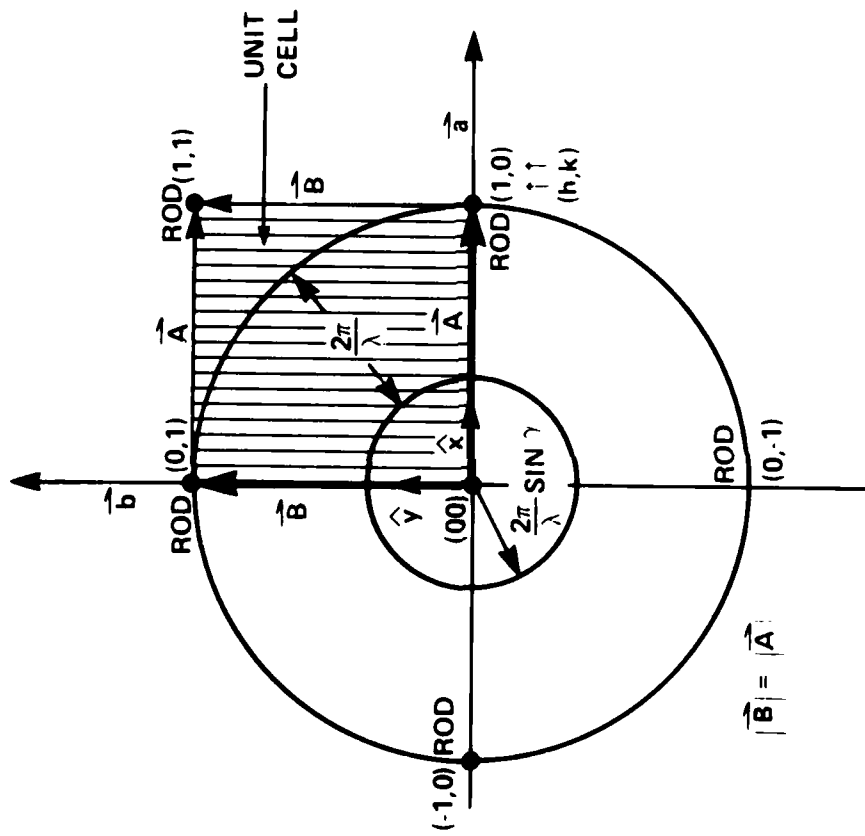


Figure 4. OPTIMUM RECTANGULAR RECIPROCAL LATTICE FOR CONICAL SCAN

for which $\vec{C} = \hat{Z}$ is assumed just for convenience in carrying out the inverse transformation of equation (10).

If the reciprocal net is hexagonal in configuration, as shown in figure 5, an optimum set of primitive vectors is,

$$\vec{A} = \frac{\pi\sqrt{3}}{\lambda} (1 + \sin\gamma) \hat{X} + \frac{\pi}{\lambda} (1 + \sin\gamma) \hat{Y} \quad (18a)$$

$$\vec{B} = \frac{-\pi\sqrt{3}}{\lambda} (1 + \sin\gamma) \hat{X} + \frac{\pi}{\lambda} (1 + \sin\gamma) \hat{Y} \quad (18b)$$

which transforms to the space lattice basis vectors,

$$\vec{a} = \frac{\lambda}{\sqrt{3}} (1 + \sin\gamma)^{-1} \hat{X} + \lambda(1 + \sin\gamma)^{-1} \hat{Y} \quad (19a)$$

$$\vec{b} = \frac{-\lambda}{\sqrt{3}} (1 + \sin\gamma)^{-1} \hat{X} + \lambda(1 + \sin\gamma)^{-1} \hat{Y} \quad (19b)$$

which also define a hexagonal lattice which is, however, rotated 30° with respect to the reciprocal rod lattice.

The array aperture area per element may be obtained from either the space or reciprocal lattice primitive vectors:

$$A_e = |\vec{a} \times \vec{b}| = 4\pi^2 |\vec{A} \times \vec{B}|^{-1} \quad (20)$$

For the two examples considered above,

$$\text{square; } A_e = \lambda^2 (1 + \sin\gamma)^{-2} \quad (21)$$

$$\text{hexagonal; } A_e = \frac{2\lambda^2}{\sqrt{3}} (1 + \sin\gamma)^{-2} \quad (22)$$

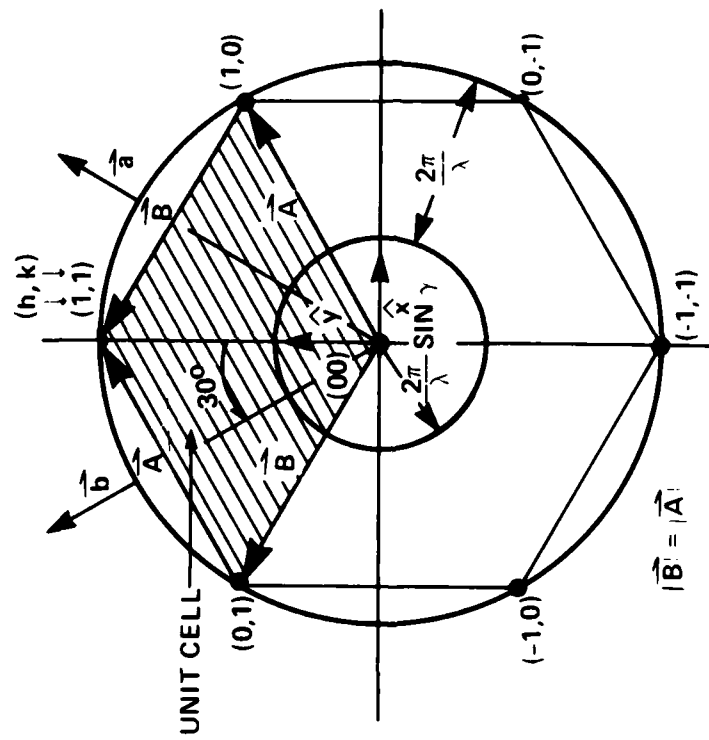


Figure 5. OPTIMUM TRIANGULAR RECIPROCAL LATTICE FOR CONICAL SCAN

and it is seen that, independent of the conical scan half angle γ , an hexagonal array lattice requires 13.4% fewer elements to fill a given aperture than a square lattice - a result which has been proven elsewhere¹.

To determine the parameters of the space lattice with the largest area per element, consistent with an absence of grating lobe peaks less than 90° off boresight for a particular field of view, the following general procedure may be employed:

- 1) The wave vectors for the specified scan boundary are projected onto the plane perpendicular to the array boresight, which is also the plane perpendicular to the reciprocal lattice rods.
- 2) The projected scan boundary is extended by radii of $(2\pi/\lambda)$ centered on each point of the scan boundary. The envelope of these circles represents the locus of all potential incipient grating lobes with peaks directed perpendicular to the array boresight, i.e., parallel to the array.
- 3) A reciprocal lattice type (triangular, rectangular, etc.) is chosen and fit to the envelope in such a way as to minimize the reciprocal lattice unit cell area ($\bar{A} \times \bar{B}$) without placing any lattice rod, save for the rod at the origin, within the envelope.
- 4) The space or element lattice is found by inverting the reciprocal lattice of step 3, using, for convenience, $\bar{C} = \hat{\lambda}$, and equations (10).

Very often the symmetry of the field of view immediately suggests an appropriate reciprocal lattice type or types for consideration. For example, if the field of view has a mirror plane of symmetry, only rectangular and isocetes triangular reciprocal lattices need be considered. Clearly, the reciprocal lattice and space lattice, should, at a minimum, have as many symmetry elements (mirror planes, rotation axes, etc.) as the field of view.

The above prescription for element lattice unit cell area maximization permits grating lobe peaks to occur parallel to the array face. However, it has been noted² that mutual coupling between the elements can cause "blind spots" when the beam is steered in a direction such that a grating lobe peak lies parallel to the array plane. To obtain the additional grating lobe suppression desired, it is usually sufficient to add one half of a full mainbeam width at the field of view boundary to the perimeter of the field of view. As explained in more detail later, this expedient places the first grating lobe null tangent to the array face.

In the following section the analysis described here is used to find the optimum element pattern for APATS.

SECTION III

ANALYSIS AND RESULTS FOR APATS

As stated in the introduction, the nominal APATS field of view, referenced to the local horizontal, is $\pm 60^\circ$ in azimuth, and from 45° to -15° in elevation. Elevation is measured in a vertical plane from the horizontal, while azimuth is measured in a horizontal plane from the vertical plane which contains the array boresight. Since the array boresight will be elevated $10^\circ - 15^\circ$ to reduce scan loss when the RV is in peak plasma, it is necessary to transform the field of view into angular coordinates referenced to the array coordinate system, in which \hat{z} lies along the boresight and \hat{x} lies in the array plane and along the horizontal. The appropriate transformation matrix and equations have been given elsewhere³ recently and will not be repeated here.

The scan boundary wave vector for the transformed field of view is projected onto the array plane in figure 6 for a boresight elevation of 10° and $\lambda = 13.3$ cm. The axes have units of cm^{-1} and this projection is actually on a reciprocal space plane parallel to the array plane. As discussed previously, the components of k which give the projection boundary are,

$$k_x = (2\pi/\lambda)\cos\theta\sin\phi = (2\pi/\lambda)\cos\alpha \quad (23a)$$

$$k_y = (2\pi/\lambda)\sin\theta = (2\pi/\lambda)\cos\beta \quad (23b)$$

in which θ and ϕ are the angular coordinates of the transformed field of view perimeter. The envelope of the $(\vec{k}' - \vec{k})$ values was produced graphically using a compass set to a radius corresponding to 0.472 cm^{-1} , the magnitude of the wave vector. Except for the

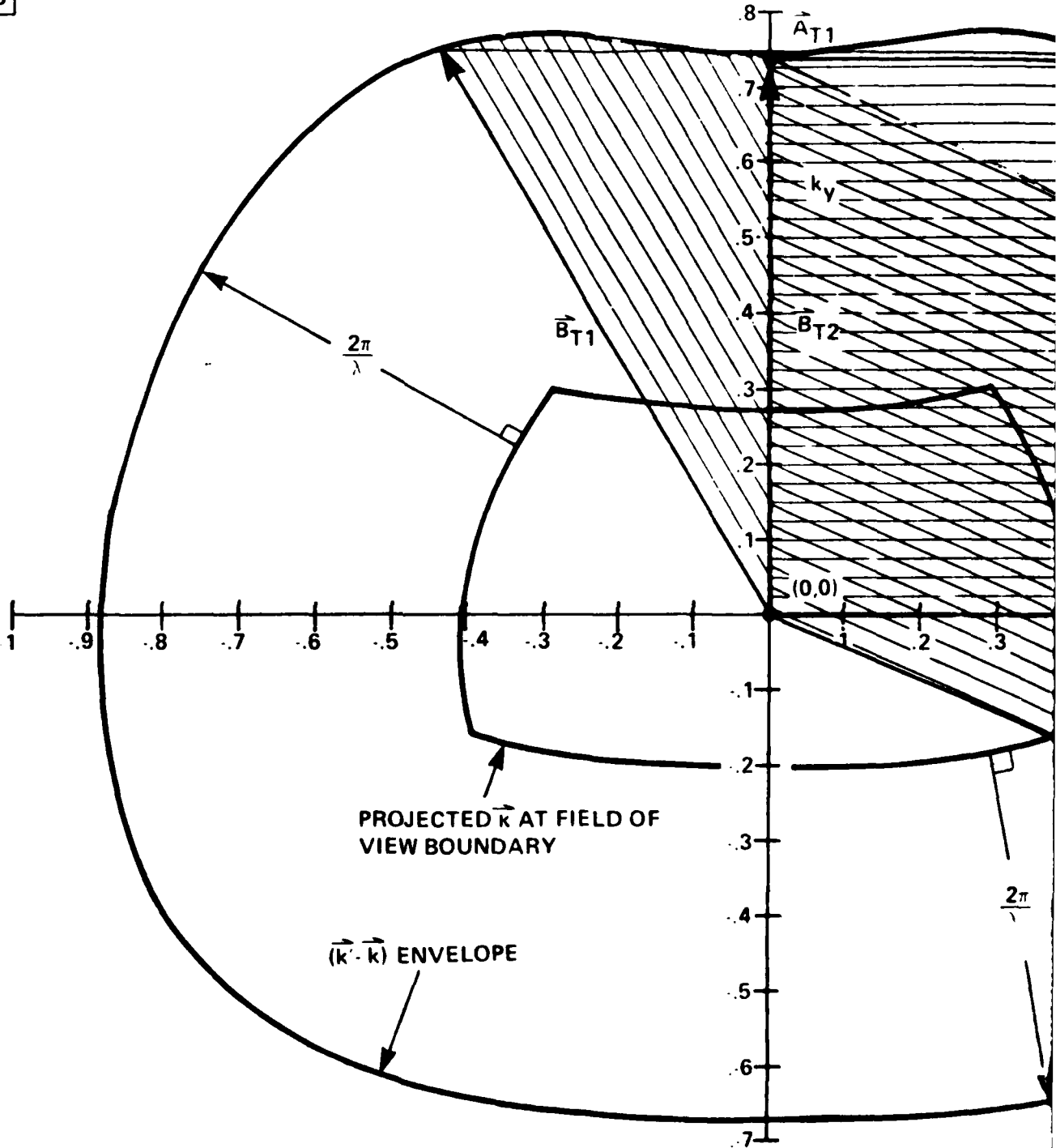
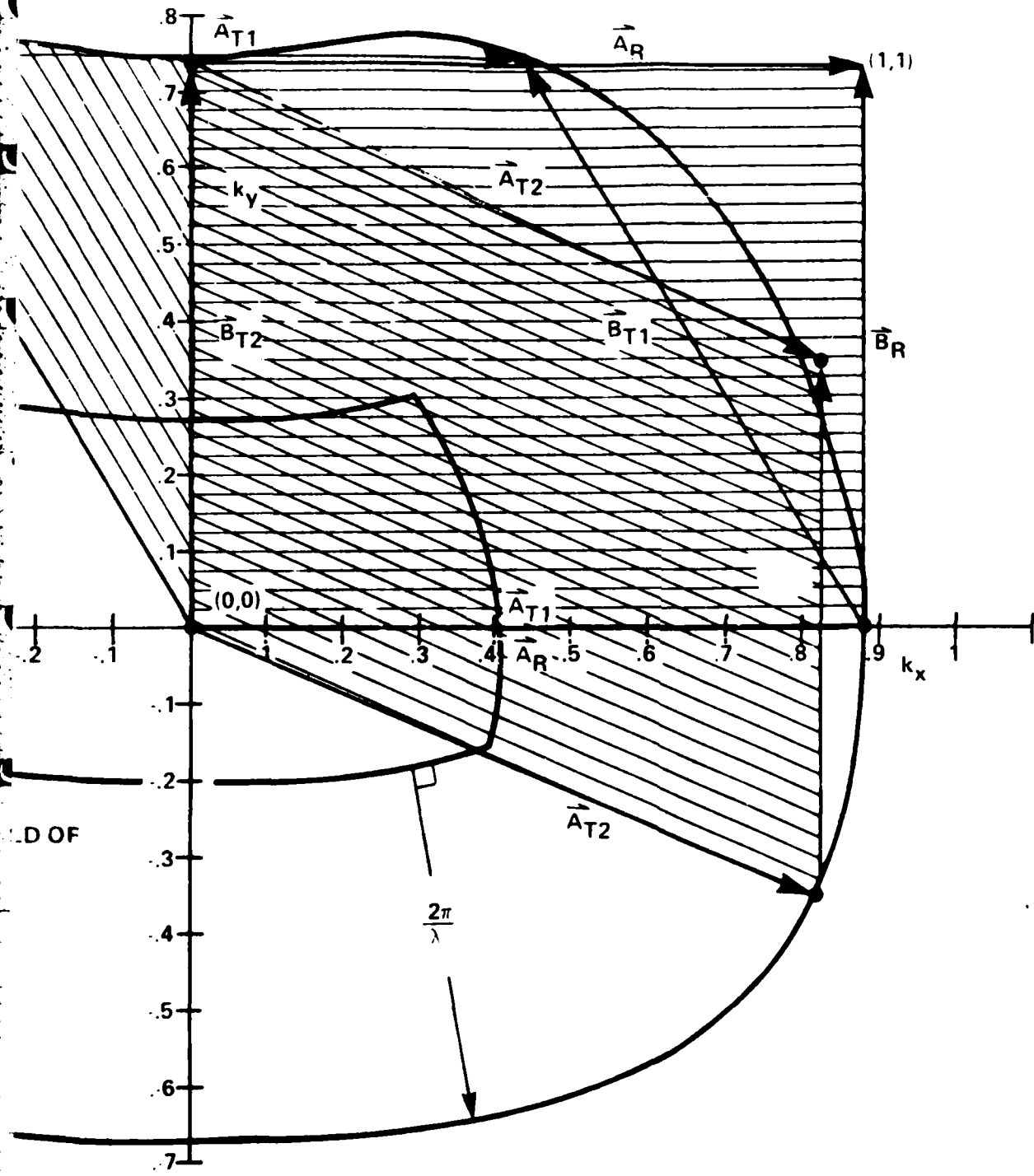


Figure 6 RECIPROCAL SPACE CONSTRUCTION FOR 10° BORESIGHT



SPACE CONSTRUCTION FOR 10° BORESIGHT ELEVATION

2

origin, the rods of the reciprocal lattice, which appear as points in the projection, must lie outside this envelope. However, the closer the rods can be spaced in reciprocal space, the larger the area will be per lattice site in the space lattice.

For a rectangular reciprocal net, the shortest primitive reciprocal lattice vectors are, in inverse centimeters,

$$\vec{A}_R = 0.880 \hat{X}, \vec{B}_R = 0.743 \hat{Y} \quad (24)$$

as illustrated in figure 6. The inverse transformation of equations (10) yields ($\vec{C} = \hat{Z}$ used for convenience),

$$\vec{a}_R = 7.14 \hat{X}(\text{cm}) = 0.537\lambda \hat{X} \quad (25)$$

$$\vec{b}_R = 8.46 \hat{Y}(\text{cm}) = 0.636\lambda \hat{Y}$$

and the space lattice is rectangular with its short dimension in the horizontal direction. The area per element is $0.342\lambda^2$ or 60.4cm^2 for $\lambda = 13.3\text{cm}$.

The symmetry of the field of view in the array coordinate system implies that only isocetes triangular lattices need be considered in addition to the rectangular lattice; however, there are two alternatives for this type of lattice:

- 1) The half width of the $\vec{k}' - \vec{k}$ envelope can be equal to twice the column separation in the reciprocal lattice.
- 2) The height of the envelope, from the origin to the top, can be equal to twice the row separation in the reciprocal lattice.

Primitive reciprocal lattice vectors for these two cases are depicted in figure 6. For case 1 these are, in inverse centimeters,

$$\vec{A}_{T1} = 0.890 \hat{X}, \vec{B}_{T1} = -0.440 \hat{X} + 0.747 \hat{Y} \quad (\text{cm}^{-1}) \quad (26)$$

and the inverse transformation produces,

$$\begin{aligned} \vec{a} &= 7.14 \hat{X} + 4.21 \hat{Y} = 0.537\lambda \hat{X} + 0.316\lambda \hat{Y} \quad (\text{cm}) \\ \vec{b} &= 8.42 \hat{Y} = 0.633\lambda \hat{Y} \quad (\text{cm}) \end{aligned} \quad (27)$$

which is a nearly hexagonal space lattice, as illustrated in figure 7. The area per element is $0.340\lambda^2$, which is slightly less than that for the rectangular lattice previously considered. Thus this triangular arrangement has no advantage over the simpler rectangular periodicity.

The second type of triangular net has primitive reciprocal vectors,

$$\vec{A}_{T2} = 0.820 \hat{X} - 0.372 \hat{Y}, \vec{B}_{T2} = 0.743 \hat{Y} \quad (\text{cm}^{-1}) \quad (28)$$

which produce the space net,

$$\begin{aligned} \vec{a} &= 7.66 \hat{X} = 0.576\lambda \hat{X} \quad (\text{cm}) \\ \vec{b} &= 3.84 \hat{X} + 8.46 \hat{Y} = 0.289\lambda \hat{X} + 0.636\lambda \hat{Y} \quad (\text{cm}) \end{aligned} \quad (29)$$

which is illustrated in figure 8. Interestingly, the area per element is $0.366\lambda^2$ - about 7% greater than that of the rectangular

IA-63,941

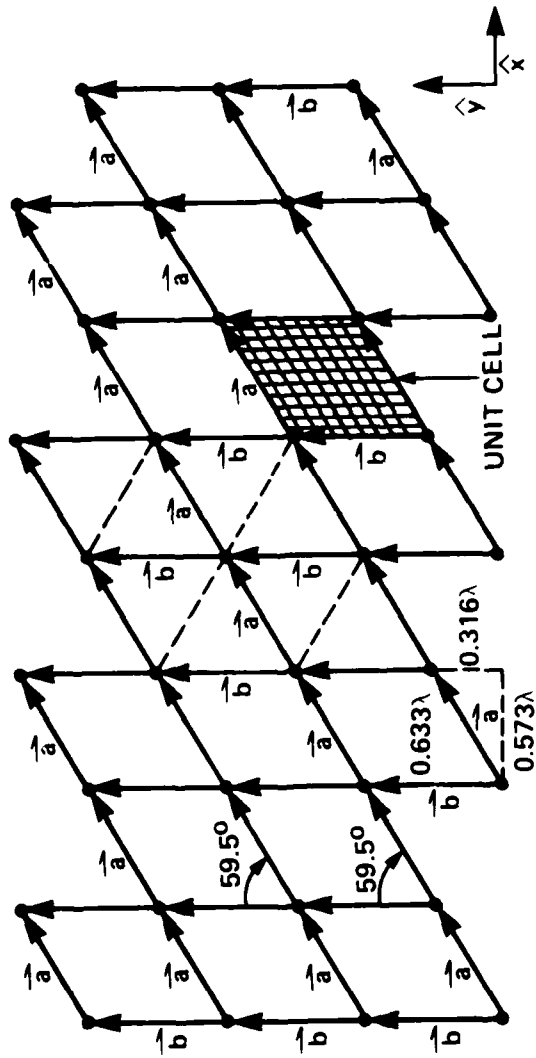


Figure 7. T1 SPACE LATTICE

IA-63,940

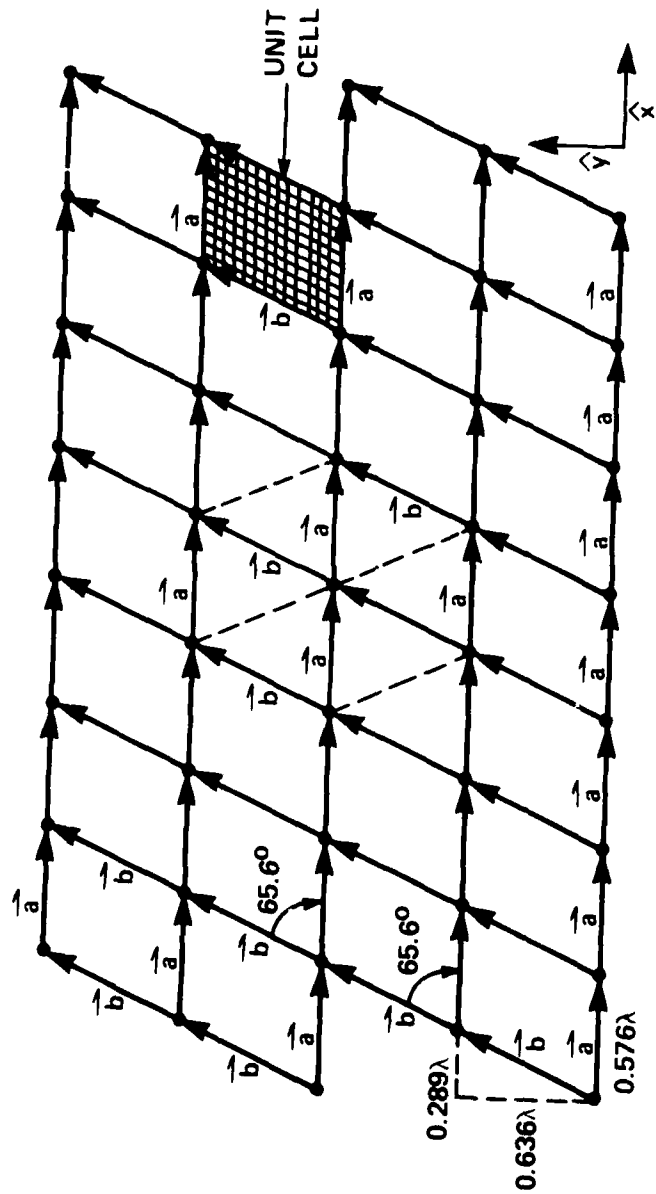


Figure 8. T2 SPACE LATTICE

lattice. This is equivalent to a 5.6% savings in elements with respect to the rectangular lattice for the field of view and boresight elevation considered.

Identical analyses have been performed for the suggested APATS field of view as transformed to an array system with a 15° boresight elevation. The salient results have been summarized in table 1, together with those pertaining to the 10° boresight elevation case just discussed. The reciprocal space construction for the 15° case appears in figure 9.

With the array boresight elevated by 15°, the projection of the transformed field of view is more nearly centered about the origin, or (0,0) reciprocal lattice rod, and it is possible to construct primitive reciprocal lattice vectors which are shorter than those required for the 10° transformed field of view. In particular, the optimum (T2) lattice for the 15° case has an area of $0.380\lambda^2$ per element - a 3.8% increase over the 10° case, which translates to 3.7% fewer elements for the 15° case. The theoretical element gain for this optimum case is,

$$G = \frac{4\pi\Lambda}{\lambda^2} = 4\pi(0.380) = 4.78 \quad (30)$$

or 6.79 dB - a value which should not be impractical; however, element scan losses must also be considered and may indicate that an element with less boresight gain and less scan loss in a tighter lattice is more desirable.

As mentioned at the end of Section II, additional grating lobe suppression may be necessary in order to reduce or avoid blind spots at those points at the field of view boundary which produce grating lobes parallel to the array. This suppression may be provided by

TABLE 1

LATTICE CHARACTERISTICS FOR APATS FIELD OF VIEW

10° Boresight Elevation

Lattice Type	$\vec{A}(\text{cm}^{-1})$		$\vec{B}(\text{cm}^{-1})$		$\vec{a}(\text{cm})$		$\vec{b}(\text{cm})$		Area Per Element (cm^2)
	\hat{x}	\hat{y}	\hat{x}	\hat{y}	\hat{x}	\hat{y}	\hat{x}	\hat{y}	
Rectangular	.880	0	0	.743	7.14	0	0	8.46	60.4 ($0.342\lambda^2$)
Triangular 1	.880	0	-.440	.747	7.14	4.21	0	8.42	60.1 ($0.340\lambda^2$)
Triangular 2	.820	-.372	0	.743	7.66	0	3.84	8.46	64.7 ($0.366\lambda^2$)

15° Boresight Elevation

Rectangular	.878	0	0	.708	7.16	0	0	8.87	63.5 ($0.359\lambda^2$)
Triangular 1	.878	0	-.439	.726	7.16	4.33	0	8.66	61.9 ($0.350\lambda^2$)
Triangular 2	.830	-.354	0	.708	7.57	0	3.78	8.87	67.2 ($0.380\lambda^2$)

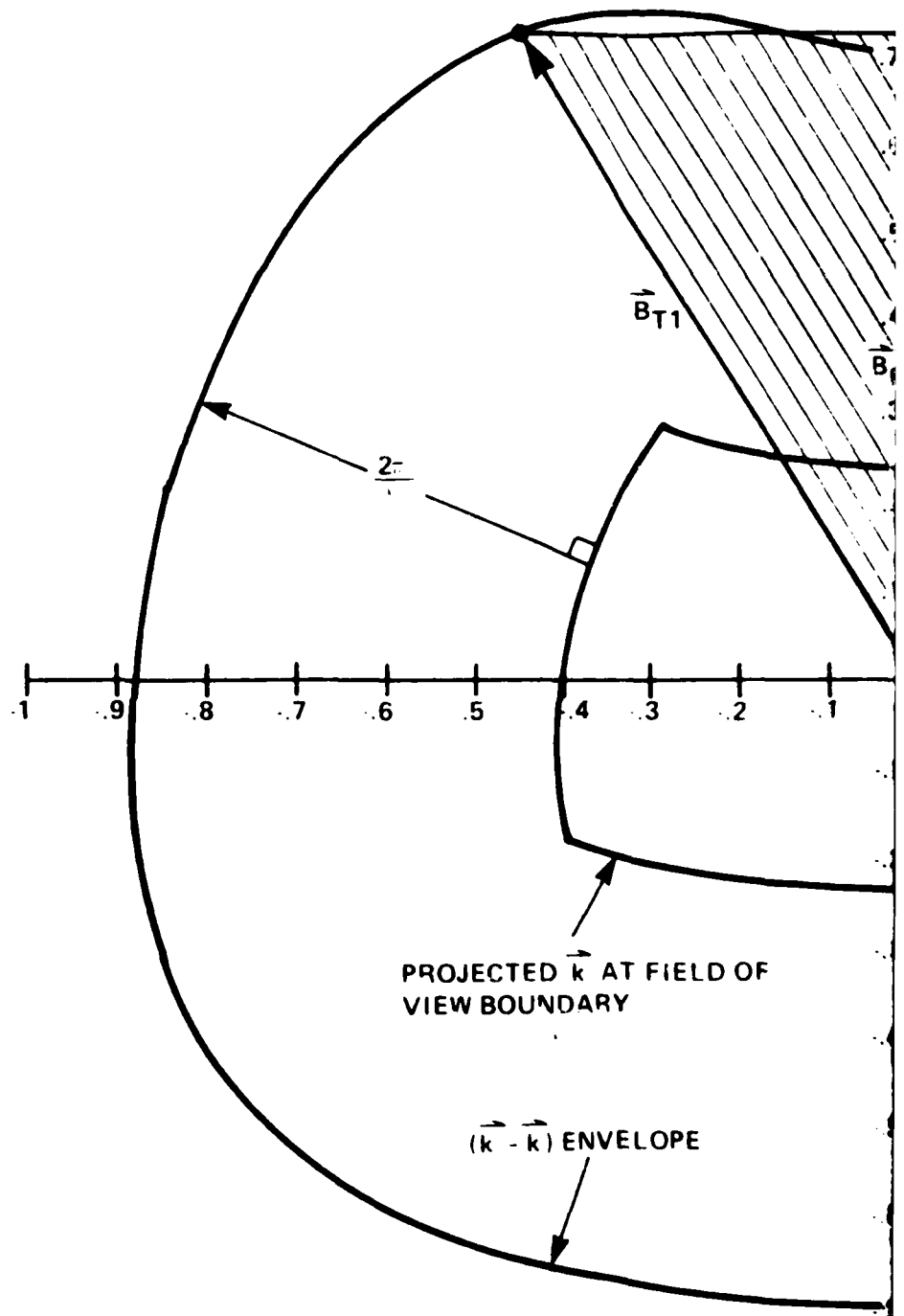
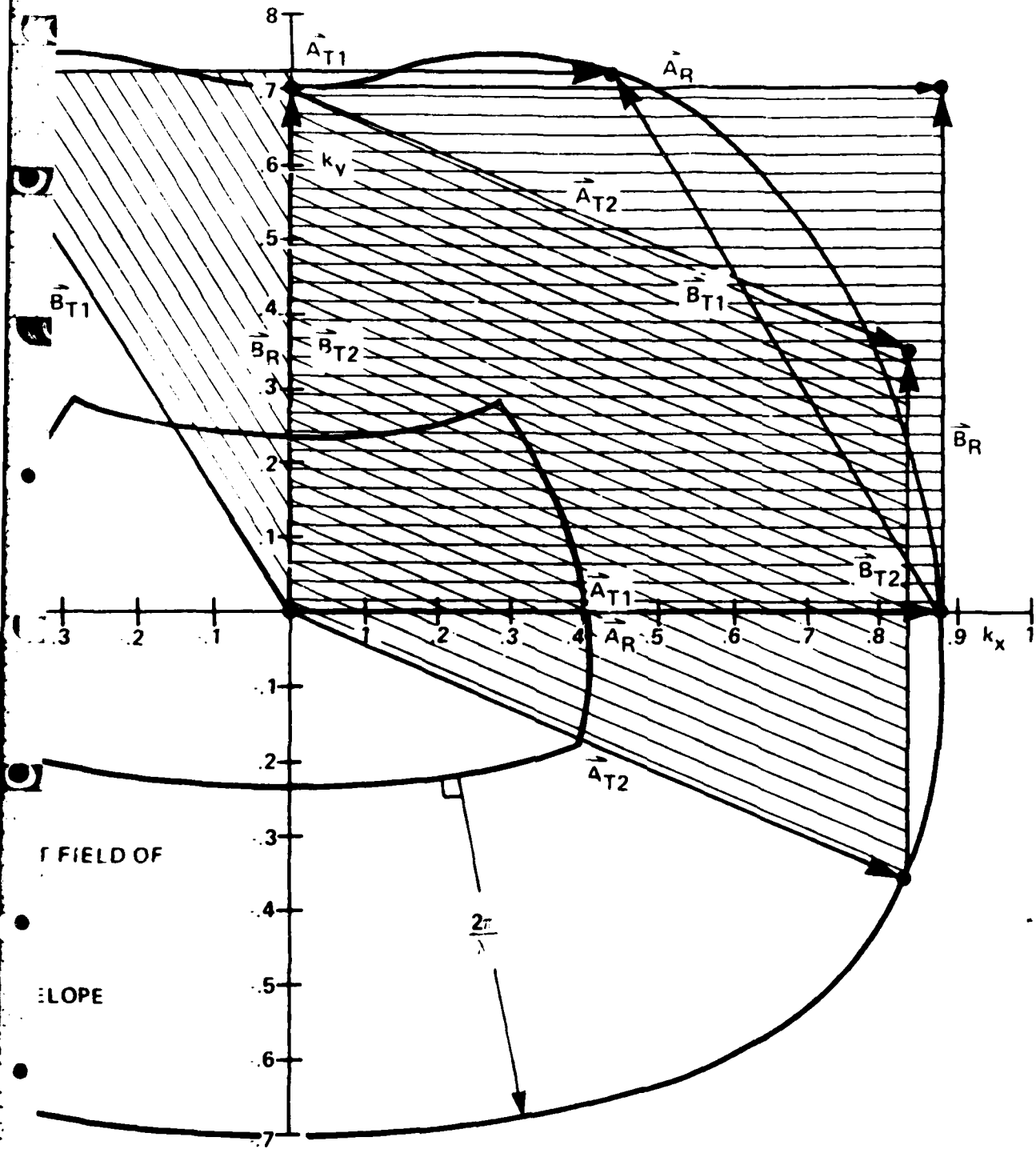


Figure 9. RECIPROCAL SPACE CONST



LOCAL SPACE CONSTRUCTION FOR 15° BORESIGHT ELEVATION

expanding the field of view in such a fashion as to place the first grating lobe null in the array plane when the main beam is steered to the original field of view boundary. The optimum lattice is determined using the expanded field of view and the procedure outlined in Section II. To a good approximation, the expanded scan area can be obtained from the specified scan area by adding one half of a full beamwidth (for a beam steered to the original boundary) to each point along the boundary. The additional scan angle is, of course, a function of scan boundary position, and array size and geometry.

The underlying principles are best illustrated by consideration of a linear array of $(N + 1)$ elements with spacing d . If the first grating lobe is parallel to the array when the beam is scanned to an angle θ' off boresight, equation (15) indicates that d must satisfy,

$$d = \lambda [1 + \sin\theta']^{-1} \quad (31)$$

If the scan angle is reduced to a value of θ , such that the phase change at any element,

$$\Delta\phi = (2\pi d/\lambda)[\sin\theta' - \sin\theta] \quad (32)$$

is equal to $2\pi/N$ radians, a null occurs in the direction where the grating lobe peak had existed when the beam was steered to θ' . Therefore, if the field of view boundary is at θ , θ' can be obtained from,

$$\theta' = \sin^{-1}[\lambda/L + \sin\theta] \quad (33)$$

in which $L = Nd$ is the length of the array. Since the grating lobe condition is satisfied at θ' , the first grating lobe null will occur

at θ as desired. Equation (33) also specifies the position of the first outside (away from boresight) null for an array beam steered to θ . Since the mainbeam is approximately symmetrical, adding half a beamwidth to the field of view should provide very nearly the desired result.

For an APATS field of view and an array which has a rectangular lattice with axes parallel to the array edges, equations (33) and (15) can be immediately used to determine the optimum lattice spacings needed to null the incipient grating lobes in the array plane. For the 10° boresight elevation case, the maximum elevation scan angle, at 0° azimuth, is increased from 35° to 39.8° , while the maximum azimuth scan, at 0° elevation, is increased from 59.6° to 65.1° as per equation (33) for an array having a width of 3m and height of 2m. The reciprocal space geometry of figure 6 indicates that only these two angular coordinates are important in the determination of the optimum element lattice. The maximum element separations can be computed by substitution of the expanded field of view angles into equation (31) or (15):

$$\bar{a} = 0.524\lambda \hat{X}, \bar{b} = 0.610\lambda \hat{Y} \quad (34)$$

The area per array element is $0.320\lambda^2$, or 6.9% less than the corresponding case without the additional suppression of the grating lobes.

For the 15° boresight elevation case, the expanded scan angles are 34.5° elevation, at 0° azimuth, and 64.5° azimuth, at 0° elevation, and the primitive lattice vectors are,

$$\vec{a} = 0.526\lambda\hat{X}, \vec{b} = 0.638\lambda\hat{Y} \quad (35)$$

which give $0.336\lambda^2$ area per element, or 6.4% less than the corresponding case without additional grating lobe suppression. Similar reductions obtain for triangular lattices, however computation for these cases is far more difficult and provides no additional insight.

SECTION 4
CONCLUSIONS

Triangular array element patterns, if properly optimized, should provide element savings of 6.5% and 5.5% for 10° and 15° boresight elevations respectively, relative to the optimum rectangular array lattices. Furthermore, it has been found that a 15° boresight elevation produces a transformed field of view which permits a reduction in element number of 3.6% compared to the 10° boresight elevation case. These results are translated into element counts for a 6m^2 array in table 2. These values should be adjusted upwards by approximately 6% if additional grating lobe suppression, as described in Section III, is used.

TABLE 2

ELEMENT COUNT VERSUS LATTICE TYPE *
(ARRAY AREA ASSUMED TO BE 6m^2)

10° Boresight Elevation

Lattice Type	Element Count
Optimum Rectangular	992
Optimum Triangular	927

15° Boresight Elevation

Optimum Rectangular	944
Optimum Triangular	893

* Grating lobe peaks are parallel to the array at maximum scan angle. Placement of first grating lobe null parallel to the array requires $\sim 6^\circ$ more elements.

LIST OF REFERENCES

1. E. D. Sharp, "A Triangular Arrangement of Planar-Array Elements that Reduces the Number Needed," IRE Trans. on Antennas and Propagation, March 1961, p. 126.
2. M. I. Skolnik, Radar Handbook, (McGraw Hill, 1970), p. 11-31, 32.
3. G. A. Robertshaw, "Frequency Dependence of APATS Antenna Gain," Appendix A, ESD-TR-82-120, Electronic Systems Division, AFSC, Hanscom AFB, MA (June 1981) (AD A115059).

APPENDIX

RECIPROCAL SPACE AND FOURIER SERIES

As is well known, a function which is piecewise continuous and periodic with period "a" can be expanded in a Fourier Series. In one dimension, the series has the exponential form,

$$f(x) = C(h) \sum_{h=-\infty}^{\infty} \exp[i \frac{2\pi h}{a} x]; \quad (h, \text{ integer}) \quad (36)$$

with coefficients,

$$C(h) = \frac{1}{a} \int_0^a f(x) \exp[-i \frac{2\pi h}{a} x] dx \quad (37)$$

If the function is defined on \vec{R} and has periodicity given by the translation vectors \vec{a} , \vec{b} and \vec{c} which lie along the \hat{X} , \hat{Y} , and \hat{Z} directions, respectively, the expansion is readily generalized to,

$$f(\vec{R}) = C(h,k,l) \sum_{h=-\infty}^{\infty} \sum_{k=-\infty}^{\infty} \sum_{l=-\infty}^{\infty} e^{i \frac{2\pi h}{|a|} x} e^{i \frac{2\pi k}{|b|} y} e^{i \frac{2\pi l}{|c|} z}; \quad (38)$$

(h,k,l integers)

Which has the required translational invariance,

$$f(\vec{R}) = f(\vec{R} + n\vec{a} + p\vec{b} + m\vec{c}) \quad (n,p,m \text{ integers}) \quad (39)$$

For convenience, equation (38) can be reexpressed,

$$f(\vec{R}) = C(\vec{K}_{h,k,l}) \sum_{h,k,l} e^{i \vec{K}_{h,k,l} \cdot \vec{R}} \quad (40)$$

where,

$$\vec{K}_{h,k,l} = h \frac{2\pi}{|a|} \hat{x} + k \frac{2\pi}{|b|} \hat{y} + l \frac{2\pi}{|c|} \hat{z} \quad (41)$$

is the set of reciprocal lattice vectors which correspond to the orthogonal set \vec{a} , \vec{b} , and \vec{c} . If these translation vectors are now allowed to represent a general (non-orthogonal) periodicity of $f(\vec{R})$ the Fourier expansion must still be invariant when \vec{R} is replaced by,

$$\vec{R} + \vec{R}_{npm} = \vec{R} + n\vec{a} + p\vec{b} + m\vec{c} \quad (42)$$

Therefore,

$$\begin{aligned} f(\vec{R}) &= f(\vec{R} + \vec{R}_{npm}) = C(\vec{K}) \sum_{\vec{K}} e^{i\vec{K} \cdot \vec{R}} \\ &= C(\vec{K}) \sum_{\vec{K}} e^{i\vec{K} \cdot \vec{R} + i\vec{K} \cdot \vec{R}_{npm}} \\ &= C(\vec{K}) \sum_{\vec{K}} e^{i\vec{K} \cdot \vec{R}} e^{i\vec{K} \cdot \vec{R}_{npm}} \end{aligned} \quad (43)$$

which is satisfied if,

$$\vec{K} \cdot \vec{R}_{npm} = 2\pi n \quad (n, \text{integer}) \quad (43)$$

which is identical to equation (5). As was demonstrated in Section II, \vec{K} must be a reciprocal lattice vector for equation (44) to be satisfied, and Fourier expansion of a function which is periodic in three dimensions therefore requires only reciprocal lattice vectors:

$$f(\vec{R}) = C(\vec{G}_{h,k,l}) \sum_{\vec{G}_{h,k,l}} e^{i\vec{G}_{h,k,l} \cdot \vec{R}}$$

In which,

$$C(\vec{G}_{h,k,l}) = \frac{1}{V} \int_V f(\vec{R}) e^{-i\vec{G}_{h,k,l} \cdot \vec{R}} dV$$

where integration is performed over the volume of the unit cell formed by the chosen set of primitive translation vectors used to specify the periodicity of $f(\vec{R})$. If $f(\vec{R})$ is a space lattice defined by a Dirac Delta Function at each site, all of the Fourier expansion coefficients are unity and it is evident that the reciprocal lattice is the Fourier transform of the space lattice.